The effect of water content on time domain dielectric response in polyetheretherketone

Torbjørn Andersen Ve, Øystein L. Hestad and Sverre Hvidsten

***Abstract*— Polyetheretherketone (PEEK) is commonly used in power connectors due to its excellent mechanical and electrical properties. In submarine electrical components, water molecules can diffuse through polymeric sealings and interfaces and finally increase the humidity in the main electrical insulation system. To examine the effect of water sorption on the dielectric properties of a semi-crystalline commercially available PEEK, polarization and depolarization currents were measured on samples preconditioned in a climate chamber to either a dry state or to a water concentration of 5000 ppmw at 30, 60 and 90 °C. The water absorption process was characterized and found to follow Fick's law, with the solubility decreasing with increasing temperature. The absorption of water was found to strongly increase the electrical conductivity. At 90 °C the conductivity increased by 85 times compared to the value measured on dry conditioned samples. The conductivity of dry PEEK also increases less with temperature than that of wet PEEK, indicating a lower activation energy in the absence of water molecules. The conduction mechanism in wet PEEK insulation is likely ionic hopping.**

***Index Terms*— Conductivity, dielectric response, diffusion processes, plastic insulation, subsea high voltage connectors, subsea power cables, water.**

I. Introduction

Polyetheretherketone (PEEK) is a commonly used insulation material in subsea power connectors due to its excellent mechanical and electrical properties. While the main concern of wet-mate connectors is the constant threat of water ingress, the effect of water on the dielectric properties is less known. Water ingress can either happen due to water vapour diffusion through polymeric sealings or due to liquid water entering during mating or de-mating. In this paper, the investigation focuses on a sealed connector, where only water having diffused through the seals is present. To pressure compensate a wet-mate connector, an electrically insulating liquid is used to fill all spaces in the design and will absorb the migrated water. This liquid will also be a part of the electrical insulation system but not an effective water barrier protecting the electrical stressed solid insulation. The increased water content in the liquid will lead to water transport into the solid PEEK material due to water vapour pressure gradients [1].

Water absorption can increase the electrical conductivity and the dielectric losses of an insulation material [2]–[6]. Changes in the conductivity may cause undesired electrical field enhancements at critical parts of the connector, especially for DC applications. In addition, water can also influence the long-term ageing performance of the insulation system [7], [8]. If the effect is significant, uncovering the conduction mechanism may give input to which design changes are necessary for mitigation. Performing dielectric response and electrical conductivity measurements of PEEK in dry conditions have been found important, as PEEK is also used other electrical components where the dielectric insulation may be subjected to radiation, chemicals and/or high temperatures [9]–[12]. The main purpose of this work has been to investigate water sorption and its effects on the conductivity and the dielectric response of PEEK.

II. Theory

As water ingress in non-porous polymers such as PEEK is a diffusion process, a brief outline of the theory for absorption and diffusion of water in solid materials is given first. Some fundamental conductivity models, as well as the likely effect of water on electrical conductivity, are reviewed. Finally, the theory on dielectric response of solid dielectrics and how the conductivity and the dielectric response function can be derived from polarization and depolarization current measurements is presented.

A. Water Sorption and diffusion

For non-porous polymers such as PEEK, water will be absorbed into free volume voids, present in the polymer due to the folding of the polymer chains. The water concentration, C, just inside the surface of the polymer will be proportional to the water partial vapour pressure, p, just outside the surface [1]:

$$C = Sp \tag{1}$$

in which S is the solubility coefficient. The maximum amount of water absorbed in a sample is given by $C_S = Sp_S$, where p_S is the vapour pressure of pure water.

The continual thermal motion of the polymer chains means that free volume is constantly redistributed, providing paths that the water molecules can move through. The net movement can be expressed by Fick's law [13]:

This work is funded by the project “High Voltage Subsea Connections (SUBCONN)”. The project is supported by The Research Council of Norway (Project No. 228344/E30), and by the following industrial partners: ABB AS, Aker Solutions AS, SCM, Chevron Norge AS, Aker BP, Nexans Norway AS, Shell Technology Norway AS and Equinor.

Torbjørn Andersen Ve (e-mail: torbjornandersen.ve@sintef.no), Øystein L. Hestad (e-mail: oystein.hestad@sintef.no), and Sverre Hvidsten (sverre.hvidsten@sintef.no) are all with SINTEF Energy Research, NO-7465 Trondheim, Norway

TABLE I

Field and temperature dependence of Schottky, Poole-Frenkel and hopping conduction mechanisms [16]. For each mechanism, a) is the original equation describing the mechanism and b) is used for curve fitting. c) is the logarithmic error function used to calculate the square sum of errors.

Conduction mechanism	Equation
Schottky injection	a) $\sigma = \frac{4\pi em(1-R)k_B^2T^2}{h^3E}\exp\left(-\frac{\Phi}{k_BT}\right)\exp\left(\beta_s\sqrt{E}\right)$ b) $\sigma = \frac{AT^2}{E}\exp\left(-\frac{B}{k_BT}\right)\exp\left(\frac{C\sqrt{E}}{T}\right)$
Poole-Frenkel	a) $\sigma = \sqrt{N_{eff}N_D}e\mu\exp\left(-\frac{\Phi}{2k_BT}\right)\exp\left(\frac{\beta_{PF}}{T}\sqrt{E}\right)$ b) $\sigma = A\exp\left(-\frac{B}{k_BT}\right)\exp\left(\frac{C\sqrt{E}}{T}\right)$
Hopping conduction	a) $\sigma = \frac{2qn_qa\nu}{E}\exp\left(-\frac{W}{k_BT}\right)\sinh\left(\frac{qaE}{2k_BT}\right)$ b) $\sigma = \frac{A}{E}\exp\left(-\frac{B}{k_BT}\right)\sinh\left(\frac{CE}{k_BT}\right)$
Square sum of errors	c) $S(A,B,C) = \sum_{T,E}\left(\log\left(\sigma_c(T,E,A,B,C)\right) - \log\left(\sigma_m(T,E)\right)\right)^2$

$$J = -D\nabla C \quad (2)$$

where J is the flux of water, and D is a proportionality coefficient called the diffusion coefficient. Rewriting (2) using the continuity equation, the time dependence can be expressed as [13]

$$\frac{\partial C}{\partial t} = -\nabla \cdot (-D\nabla C) \quad (3)$$

where t is time. As can be seen from (1) and (3), knowing D and S will give an accurate description of water uptake and transport in a polymer.

In order to determine S and D, the mass uptake of water at different temperatures can be measured. By solving (3), the relation between mass uptake and the solubility and diffusion coefficients for a thin film sample can be found [14]. This can be expressed as

$$C(t) = C_S\left(1 - exp\left(-7.3\left(\frac{Dt}{l^2}\right)^{3/4}\right)\right) \quad (4)$$

where l is the sample thickness.

The transport of water through a film is called permeation. For a film of thickness l with water vapour pressure p_2 on one side and p_1 on the other, where $p_2 > p_1$, the water flux, also called the water vapour transmission rate, through the film can be found by combining Fick's and Henry's laws, yielding

$$J = P\frac{p_2 - p_1}{l} \quad (5)$$

where $P = DS$ is the permeability coefficient.

The temperature dependencies of each of the coefficients can be assumed to follow the Arrhenius relation [15].

B. Electrical conductivity

The electrical conductivity of materials is proportional to the product of charge carrier density and carrier mobility, both of which can be dependent on the electric field and the temperature. The dominating charge carriers for polymer dielectrics at low fields are most often ions, typically originating from impurities [16]. At higher fields electrons may become the dominating charge carrier species due to their higher mobility. Electrons may be introduced from impurities with low ionization potential in the bulk or through injection of charge from energized metal surfaces in direct contact with the dielectric [16]. A range of physical models for the electric field dependence of injection and transport of charge carriers in dielectrics exist, and the governing equations of a few relevant models are summarized in Table I. Previously published results indicate that the dominating mechanism may be either Poole-Frenkel or hopping conduction [11], [17].

When water is dissolved in liquids or solids, it typically has a significant effect on the conductivity of the dielectric [2], [4], [5], and several explanations for this exist [5], [16], [18]–[21]. The first explanation is that water molecules can dissociate into ions [5]. As the water ions are relatively small, they have a high mobility compared to other typical impurity ions in the solid and can therefore contribute significantly to the current. The second explanation is that impurities present in polymers can dissociate into ions, a process that can be enhanced by the presence of water [18]. Finally, the third explanation is that at high electrical fields water molecules may enhance the mobility of electrons by acting as shallow traps in the dielectric [19], [20]. These shallow traps will also lower the injection barriers at metal surfaces and may thus result in an increase in both the number and mobility of electrons in the dielectric [16], [21].

C. Dielectric response

Polarization and depolarization currents can be used to analyse the low frequency response of insulation materials, which is important for slow polarization processes. The current flowing through the insulation material is given by [22]

$$I_p(t) = \left(\frac{\sigma}{\varepsilon_{DC}} + \varepsilon_\infty\delta(t) + f(t)\right)C_0U_0 \quad , \quad 0 \le t \le t_0 \quad (6)$$

where U_0 is the applied voltage in the time period between $t = 0$ and $t = t_0$, C_0 is the geometric capacitance of the sample, σ is the electrical conductivity, ε_{DC} is the DC permittivity of the sample, ε_∞ is the instantaneous permittivity, $\delta(t)$ is a delta function, and $f(t)$ is the frequency response function of the material.

The current during the depolarization phase ($t > t_0$) is given by,

$$I_d(t) = -\left(f(t - t_0) - f(t) + \varepsilon_\infty\delta(t - t_0)\right)C_0U_0 \quad , \quad t_0 < t \quad (7)$$

The formula for the depolarization current does not contain the conductivity, and is therefore convenient to use when calculating the dielectric response function, $f(t)$:

Author Accepted Manuscript version of the paper by Torbjørn Andersen Ve, Øystein Hestad and Sverre Hvidsten
in IEEE Transactions on Dielectrics and Electrical Insulation, 30 (2024) 501-508, http://dx.doi.org/10.1109/TDEI.2023.3243878

$$f(t) = \frac{I_d(t)}{C_0 U_0} + f(t - t_0) \quad , \quad 0 \le t \le \infty \tag{8}$$

Typically, the depolarization currents of most dielectric materials can be piecewise approximated with a Curie-von Schweidler model [22],

$$I_d(t) = -A\ t^{-n} \quad , \quad t > 0 \tag{9}$$

According to the Hamon approximation [23] the imaginary part of the complex susceptibility can then be obtained using

$$\left.\begin{aligned} \chi''(t) &\approx -\frac{I_d(t=t_1)}{\omega C_0 U_0} \\ \omega t_1 &= \left(\Gamma(1-n)\cos\left(\frac{n\pi}{2}\right)\right)^{-\frac{1}{n}} \approx 0.63 \end{aligned}\right\} \quad 0 < n < 2 \tag{10}$$

where I_d is the dipole current, C_0 the geometric capacitance, ω the angular frequency, U_0 the applied voltage, and t_1 the time the measurement is recorded at.

III. EXPERIMENTAL SETUPS AND PROCEDURES

A. Sample material

All samples were taken from the same 250 µm thick medium-viscosity, unreinforced, semi-crystalline PEEK film, obtained from a commercial manufacturer. The samples were preconditioned by drying in vacuum at 80°C for at least 3 days.

The crystallinity of the PEEK was determined by differential scanning calorimetry (DSC) measurements. The samples were heated at 10 K/min from 25 to 400 °C (above the melting point of PEEK). The crystallinity was calculated from the measured melting endotherm, using 130 J/g as the PEEK heat of fusion [24]. The crystallinity of the samples was found to be 35±2 %. The glass transition temperature was measured to be 145 °C.

B. Water absorption and Permeability

Water absorption measurements were performed by using an ultra-sensitive balance (Mettler Toledo UMX2). Sample discs, 25 mm in diameter, were prepared and dried. The mass of the samples was measured, before the samples were placed in containers filled with de-ionised water at 30, 60, and 90 °C. De-ionised water was chosen as this is equivalent to the type of water present in a sealed connector. The mass of the samples was measured at given intervals, and the concentration of absorbed water calculated from the mass increase. Measurements continued for an extended period to ensure equilibrium was reached, i.e. no significant change of average concentration for several consecutive measurements, making the total measurement period 28 days for 90 °C, 48 days for 60 °C, and 69 days for 30 °C. The solubility and diffusion coefficients were determined through equations (1) and (4).

To determine the permeability coefficient, the water vapour transmission rate was measured using a commercial analyser (Systech Illinois M7001), consisting of an upper and a lower chamber separated by the sample film. Wetted nitrogen was passed through the upper chamber, while dry nitrogen was passed through the lower chamber, setting up a known concentration gradient across the film. A phosphor-pentoxide absorption sensor was used to measure the water content in the dry nitrogen. The measurement temperature was 30 °C, and measurements were performed at 20 and 80 % relative humidity.

The temperature dependence of the permeability of PEEK was found by using a permeability cell and the freeze-drying method [25]. A heated water reservoir provided a constant high partial pressure on one side of the film, while a vacuum pump kept the partial pressure near zero on the other side. Water permeated through the sample due to the concentration gradient and was collected in a cold trap. By closing off the volume around the cold trap from the rest of the system and heating the cold trap, the amount of permeated water was measured. The water flux, and thereby the permeability coefficient, was calculated by using measurements at different time intervals. Measurements were performed at 30, 60 and 90 °C.

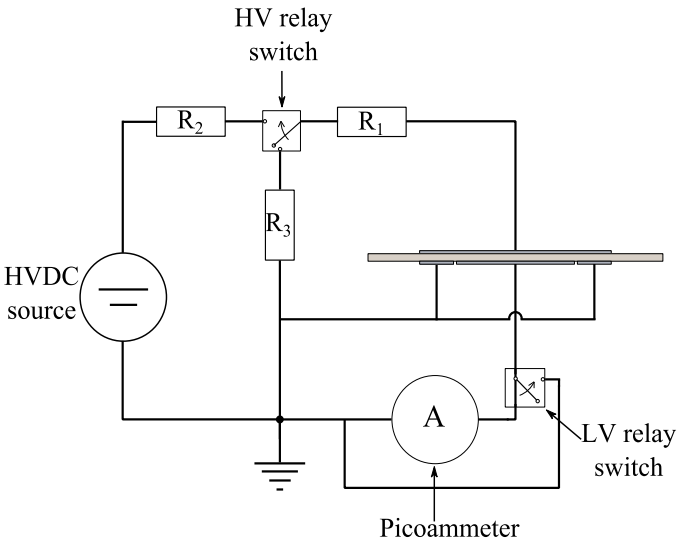

Fig. 1 Schematic of the polarization and depolarization current measurement setup. The sample is seen on the right side of the drawing. The HV and LV relay switches are used to switch between charging and discharging the samples and for protecting the picoammeter respectively.

C. Polarization and depolarization currents

Current measurements were performed on disc samples, 10 cm in diameter, with a circular high voltage electrode on one side, and concentric measure and guard electrodes on the other. All three electrodes were made by vacuum deposition of aluminium on the sample.

The experimental setup is shown schematically in Fig. 1. When measuring charging currents, the sample was connected to a high-stability HVDC source through two resistors, and the current was measured by a picoammeter (Keithley 6485). After 1 hour, the high voltage relay switched the sample's high voltage electrode to ground, and the resulting discharging current was measured. The low voltage relay switch grounded the measurement input of the picoammeter during switching of the high voltage relay, to protect the picoammeter. The polarization and depolarization periods were 1 hour each, with a wait-time between charging periods of at least 10 hours (during which all electrodes were grounded).

Author Accepted Manuscript version of the paper by Torbjørn Andersen Ve, Øystein Hestad and Sverre Hvidsten
in IEEE Transactions on Dielectrics and Electrical Insulation, 30 (2024) 501-508, http://dx.doi.org/10.1109/TDEI.2023.3243878

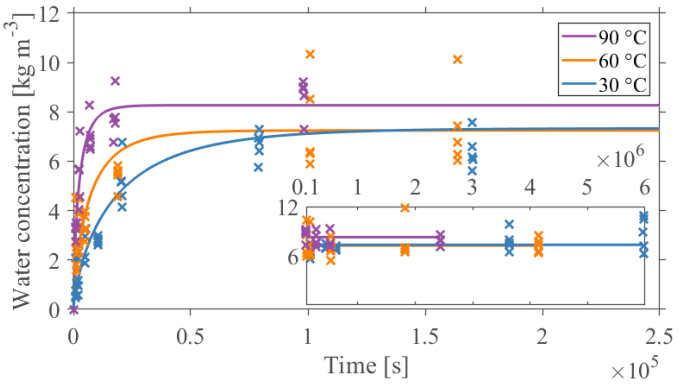

Fig. 2. Results from water absorption measurements, with the main figure showing the first 3 days of measurement, and the inset showing the results from 3 days onwards. The crosses are the individual measurements, the lines are fits to (4).

The conductivity of the samples can be found by combining equations (6) and (7):

$$I_p + I_d = \frac{\sigma}{\varepsilon_{DC}} C_0 U_0 \tag{11}$$

The conductivity was evaluated by using the average value of the last half hour of the charging and discharging currents. This assumes that the charging period has been long enough that $f(t-t_0)=0$ is a good approximation. Solving equation (11) for the conductivity, and inserting values for the currents and the geometric capacitance of the sample, $C_0 = \varepsilon_{DC}\frac{\pi r^2}{l}$, where r is the radius of the measurement electrode, yields

$$\sigma = \varepsilon_{DC}\frac{I_p+I_d}{U}\frac{l}{\pi r^2} \tag{12}$$

All dielectric response measurements were performed at a constant water concentration in the samples. Two concentrations were applied: Either dry or wet (5000 ppm_w). The test cell was placed in a climate chamber to regulate the ambient relative humidity and temperature. Conditioning times and levels of relative humidity required to obtain 5000 ppm_w in the samples were calculated by using the diffusion- and solubility coefficients found in the water absorption and permeability measurements.

IV. Experimental Results and Discussion

A. Water absorption

The results from the water absorption measurements are shown in Fig. 2. To improve readability, the figure only shows the first 3 days of measurements. The rate of water absorption increases with increasing temperature, while the maximum amount of water absorbed seems to be unchanged from 30 to 60 °C, and increases from 60 to 90 °C. The equilibrium amount absorbed, 7-8 kg m^{-3}, is close to what was found for injection-moulded semi-crystalline PEEK in [26]. This is very high when compared to a traditional high voltage insulation material such as XLPE, which absorbs less than 0.4 kg m^{-3} in the same conditions[23].

The measured results were found to correspond well with the fitted curves, indicating that the absorption process follows Fick's law. This is in accordance with earlier results in the literature which found PEEK to be a Case I Fickian material [26]. The solubility of PEEK, as found in the measurements, decreases with increasing temperature, yielding coefficients very similar to [26]. This reflects the small difference between water absorption saturation levels at different temperatures typical of polymers below their glass transition temperature due to only small changes in free volume occurring with changing temperature. The diffusion coefficient increases with temperature, with an activation energy lower than reported in [26]. It is possible that this is an effect of the slightly higher crystallinity of the PEEK used here, 35 % compared to the 30 % in [26], due to higher chain restriction limiting the movement of water molecules. The permeability, calculated from the product of the diffusion and solubility coefficients, is almost independent of temperature.

The solubility and diffusion coefficients at each individual temperature was found through curve fitting of equation (4), with the results being presented in Table II. Arrhenius relations were used to quantify the temperature dependencies of the diffusion and solubility coefficients, the results of which are shown in Table III.

Table II

Solubility and diffusion coefficients from absorption measurements, and the calculated apparent permeability.

T	S	D	$P = DS$
[°C]	[kg m^{-3} Pa^{-1}]	[m^2 s^{-1}]	[kg m^2 s^{-1} m^{-3} Pa^{-1}]
30	$1.73\cdot10^{-3}$	$9.43\cdot10^{-13}$	$1.63\cdot10^{-15}$
60	$3.64\cdot10^{-4}$	$2.47\cdot10^{-12}$	$8.98\cdot10^{-16}$
90	$1.18\cdot10^{-4}$	$6.77\cdot10^{-12}$	$7.99\cdot10^{-16}$

Table III

Arrhenius coefficients calculated based on the absorption measurements.

S_0	[kg m^{-3} Pa^{-1}]	$1.43\cdot10^{-10}$
E_S	[J mol^{-1}]	$-4.10\cdot10^{4}$
D_0	[m^{-2} s^{-1}]	$1.32\cdot10^{-7}$
E_D	[J mol^{-1}]	$2.99\cdot10^{4}$

Table IV

Average water vapour transmission rate and permeability of PEEK.

RH	WVTR	P
[%]	[kg m^{-2} s^{-1}]	[kg m^2 s^{-1} m^{-3} Pa^{-1}]
22	$3.81\cdot10^{-9}$	$1.01\cdot10^{-15}$
83	$1.66\cdot10^{-8}$	$1.15\cdot10^{-15}$

Author Accepted Manuscript version of the paper by Torbjørn Andersen Ve, Øystein Hestad and Sverre Hvidsten
in IEEE Transactions on Dielectrics and Electrical Insulation, 30 (2024) 501-508, http://dx.doi.org/10.1109/TDEI.2023.3243878

Table V

Average water flux and permeability from liquid water permeability measurements

T	J	P
[°C]	[kg m^{-2} s^{-1}]	[kg m^{2} s^{-1} m^{-3} Pa^{-1}]
30	$4.01 \cdot 10^{-8}$	$2.23 \cdot 10^{-15}$
60	$1.84 \cdot 10^{-7}$	$2.20 \cdot 10^{-15}$
90	$6.85 \cdot 10^{-7}$	$2.34 \cdot 10^{-15}$

Comparing the findings in Table II and Table III to results from measurements on XLPE found in [25], it is seen that PEEK has a much higher solubility. This is likely due to that the polar groups in PEEK monomers makes water attach more easily to PEEK polymer chains, compared to the non-polar XLPE chains. The diffusion coefficient, on the other hand, is much lower in PEEK than in XLPE, an effect of the lower chain mobility of PEEK being below its glass transition at the measurement temperatures. In comparison, XLPE is above the glass transition in the same temperature range and therefore has more flexible chains.

The average water vapor transmission rate (WVTR) at 22 and 83 % RH is given in Table IV. Looking at the effect of temperature on the water permeability, see Table V and Table VI it is found to increase slightly with temperature, having an activation energy of 738 J/Kmol. The low activation energy reflects a permeability that changes very little with temperature, similar to what was found in the absorption measurements, albeit with a positive rather than a negative activation energy. The different signs on the permeability activation energies are

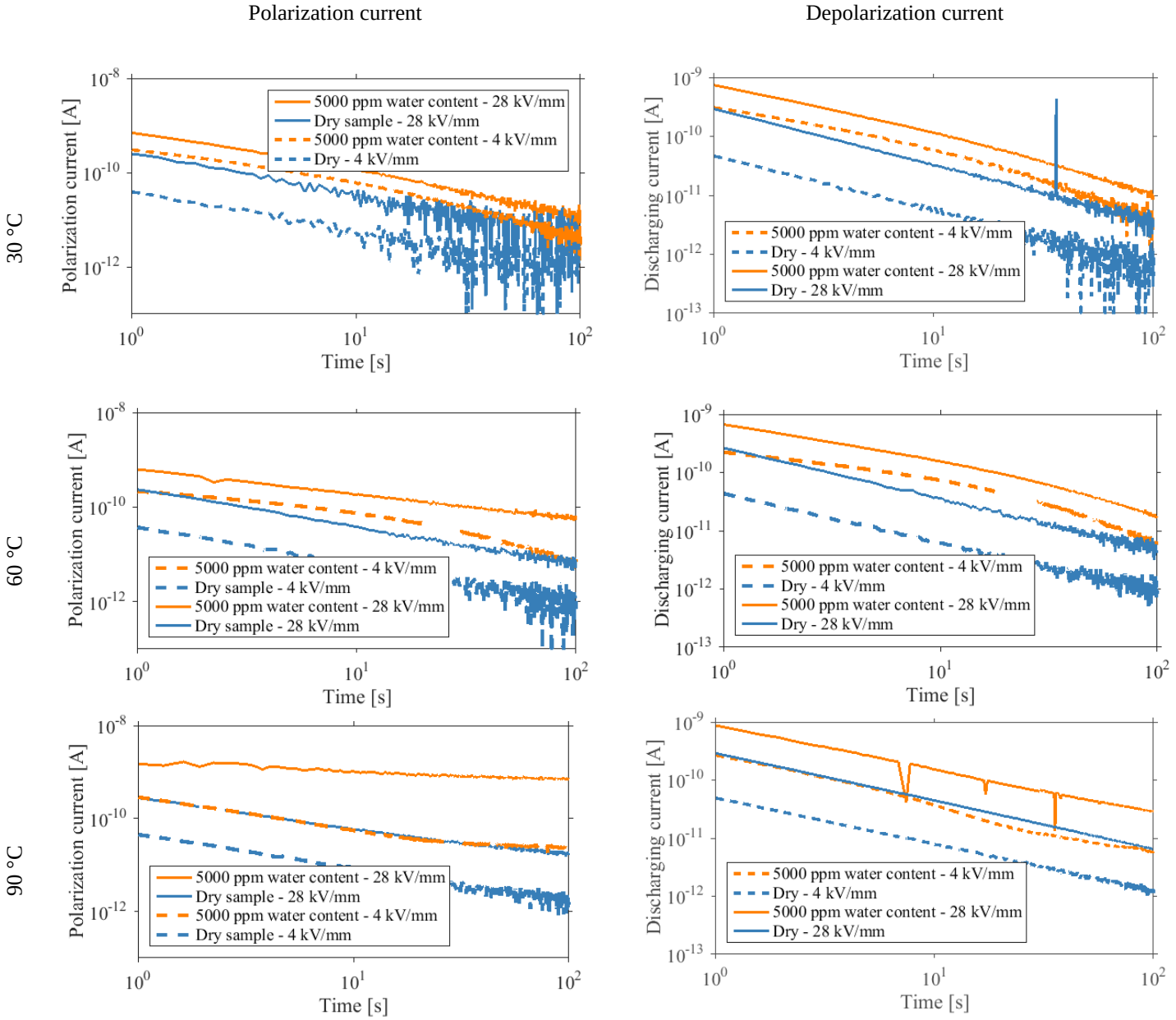

Fig. 3. Polarization (left) and depolarization (right) currents at 30, 60, and 90 C (top to bottom) and at 1 and 7 kV applied electric potential over the sample (4 and 28 kV/mm).

Author Accepted Manuscript version of the paper by Torbjørn Andersen Ve, Øystein Hestad and Sverre Hvidsten
in IEEE Transactions on Dielectrics and Electrical Insulation, 30 (2024) 501-508, http://dx.doi.org/10.1109/TDEI.2023.3243878

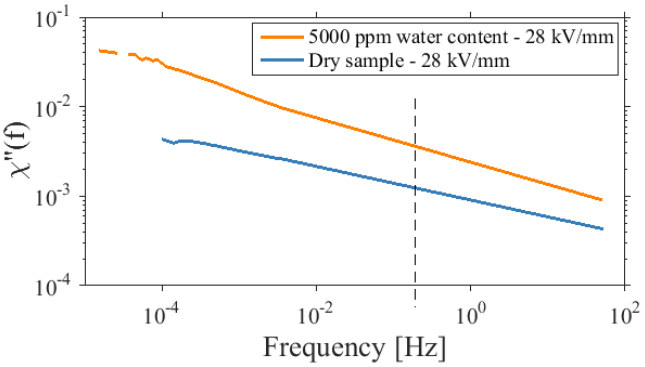

Fig. 4. Imaginary electrical susceptibility versus frequency at 90 °C. Calculated using the Hamon approximation. Results shown for frequencies above the dotted lines are based on extrapolation.

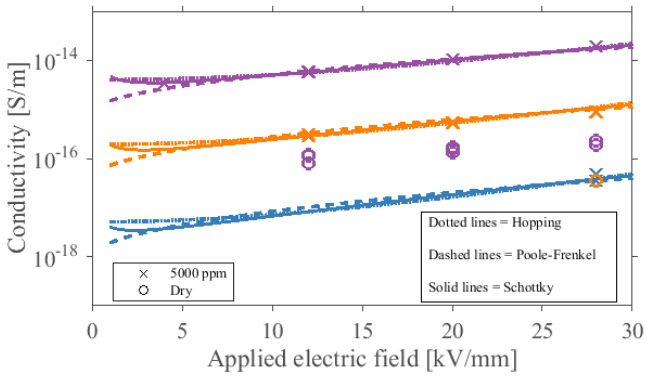

Fig. 5. Conductivity measured on dry samples and samples with increased water content. The markers are conductivities calculated from the measurements, the lines are fits to Schottky injection, Poole-Frenkel

probably a consequence of the temperature dependence being too low to accurately determine with the measurement methods.

Table VI
Arrhenius coefficients from liquid water permeability measurements

P_0	[kg m^2 s^{-1} m^{-3} Pa^{-1}]	$2.95 \cdot 10^{-15}$
E_P	[J mol^{-1}]	$7.38 \cdot 10^{2}$

B. Polarization and depolarization currents

In the following, some key experimental results showing the effect of humidity, electric field and temperature on the recorded polarization and depolarization currents are given. To improve readability of the figures only the results for 1 and 7 kV are presented (corresponding to 4 and 28 kV/mm respectively), which represents the minimum and maximum voltage applied to the samples.

The general trend is that both polarization and depolarization currents form straight lines in a log-log plot, see Fig. 3. This indicates that the currents can be fitted to the Curie-von Schweidler law, Equation (9). This also makes the transition from the time domain measurements to frequency domain analysis of the losses in the material at low frequencies possible by using the Hamon approximation, see Equation (10). Fig. 4 shows the calculated imaginary electrical susceptibility of PEEK versus frequency at 90 °C and 28 kV/mm. The frequency range for the calculated susceptibility is from 0.1 Hz and down to between 10^{-4} and 10^{-5} Hz, where the lower limit is given by the 1 pA noise threshold of the current measurements. Comparing the results for dry and humid samples shows very similar frequency dependence of the loss curve, with the most significant difference being that absorbed water increases the overall magnitude of the losses. There is no indication of additional loss mechanisms introduced due to water absorption in the frequency range of the measurements. Results on polymers has shown that humidity primarily influences the conductivity at low frequencies [27], which is in line with the findings on PEEK. Due to the limited number of water concentration levels in the experimental matrix, the specific dependence of the dielectric response on water concentration could not be obtained in this work.

C Conductivity

Using the results from the latter part of current measurements, the conductivity for each voltage and temperature was calculated using (12), for samples in dry conditions and samples with increased water content. The curve fitting equations are shown denoted as equations b) in Table I.

The noise level in the measurements was around 1 pA. For dry samples, no currents at 30 °C were above this level, while at 60 °C only currents at the highest voltage were above the noise level. At 90 °C, only the measured current at the lowest voltage was below the noise level. This left too few measurement points to provide a reasonable data set for fitting temperature- and electric field dependence. For samples at 5000 ppm, currents at the highest voltage were above the noise level at 30 °C, currents at the three highest voltages were above at 60 °C, and all the measured currents were above the noise level at 90 °C, meaning that a curve fit could be performed.

Fig. 5 shows the results from the measurements, as well as the curve fits. Starting with a comparison of dry and wet samples, the absorption of water increased the conductivity of PEEK to 25 times the value of the dry sample at 60 °C, and to between 50 and 85 times the value at 90 °C. The difference in conductivity at 90 °C was larger at higher voltages.

For samples with 5000 ppm water content, the results from the curve fits are shown in Table VII. All three of the mechanisms provided reasonable fits to the data set, with the Schottky mechanism having a slightly lower squared sum of errors. To investigate the validity of each mechanism further the C parameter was used to calculate the apparent relative permittivity for the Schottky and Poole-Frenkel mechanisms, and the average hopping distance for ionic hopping. For Schottky this yielded $\varepsilon_r = 1.26$, which is significantly lower than the expected value of 2.8. While earlier works also found a significantly lower ε_r for dry PEEK film compared to the expected value [11], the difference for wet PEEK is smaller. For Poole-Frenkel, $\varepsilon_r = 4.6$ for a system with no traps, and $\varepsilon_r = 18.4$ for a system with a single trap level, both of which are higher

Author Accepted Manuscript version of the paper by Torbjørn Andersen Ve, Øystein Hestad and Sverre Hvidsten
in IEEE Transactions on Dielectrics and Electrical Insulation, 30 (2024) 501-508, http://dx.doi.org/10.1109/TDEI.2023.3243878

than the expected value. In the literature, the relative permittivity calculated with a Poole-Frenkel mechanism was found to closely match values measured with other techniques for dry PEEK film [11], which means that the results for wet PEEK in this paper diverges significantly. For ionic hopping, the hopping distance was calculated to around 8 nm. This is in the same order of, but higher than, values reported in the literature for dry PEEK film [11], [17]. Looking at the activation energies, all mechanisms yield around 1 eV, as shown in Table VII. The value for the Schottky mechanism can be directly compared to earlier work, and is in the same range as the 1.3-1.4 eV reported for dry PEEK film there [17]. However, when comparing the results on wet samples and dry samples, the conductivity of dry PEEK appears to change less with temperature, indicating that the absence of water would yield a lower activation energy. There are not enough data points to do a proper calculation of this, however.

Table VII

Results from conductivity curve fitting, samples with high water content. A logarithmic error function was used as the basis to calculate the square sum of errors, shown as equation c) in Table I.

Mechanism	*A*	*B*	*C*	*S*(*A*,*B*,*C*)
	[*]	[eV]	[*]	[-]
Hopping	$3.29 \cdot 10^{7}$	1.08	$4.48 \cdot 10^{-5}$	0.24
Poole-Frenkel	$5.97 \cdot 10^{-1}$	1.07	$2.05 \cdot 10^{-1}$	0.30
Schottky	$1.84 \cdot 10^{1}$	1.09	$3.93 \cdot 10^{-1}$	0.16

* Unit depends on mechanism

In summary, none of the candidate mechanisms seem to fit significantly better for wet PEEK. All of the conduction mechanisms showed a significant change in a physical parameter compared to the expected values for dry PEEK to fit to the data; divergence in relative permittivity for Schottky and Poole-Frenkel conduction, and longer distance between jump sites for hopping conduction. Although the conduction mechanism for dry samples could not be determined in this work, in literature ionic hopping has been indicated as the most likely candidate [11], [17].

V. Conclusion

The water absorption and dielectric properties of a semi-crystalline PEEK material commonly used in subsea connectors have been examined. From the experimental results it can be concluded that:

- The diffusion and absorption of water in the PEEK material were found to be similar to results on PEEK grades previously reported in the literature.
- Water absorption in PEEK was found to increase the low-frequency losses, but not to introduce any new low-frequency loss mechanisms.
- Water absorption in PEEK was found to increase the conductivity by up to two decades, with the magnitude being temperature and electric field dependent. The conduction mechanism in wet PEEK insulation could not conclusively be determined.

Acknowledgment

We would like to thank Jostein Danielsen Kvitvang and Øystein Midttveit for performing some of the measurements while working as summer interns at SINTEF Energy Research.

References

[1] G. S. Park og J. Crank, *Diffusion in polymers*. London: Academic Press, 1968.

[2] C. Zou, J. C. Fothergill, og S. W. Rowe, «The effect of water absorption on the dielectric properties of epoxy nanocomposites», *Dielectrics and Electrical Insulation, IEEE Transactions on*, bd. 15, nr. 1, s. 106–117, 2008.

[3] T. P. Hong, O. Lesaint, og P. Gonon, «Water absorption in a glass-mica-epoxy composite-[I: Influence on Electrical Properties]», *IEEE Trns. Dielectr. Electr. Insul.*, bd. 16, nr. 1, s. 1–10, 2009.

[4] T. A. Ve, F. Mauseth, og E. Ildstad, «Effect of water content on the conductivity of XLPE insulation», presentert på Electrical Insulation and Dielectric Phenomena (CEIDP), 2012 Annual Report Conference on, okt. 2012, s. 649–653. doi: 10.1109/ceidp.2012.6378864.

[5] J. Yang, X. Wang, H. Zhao, W. Zhang, og M. Xu, «Influence of moisture absorption on the DC conduction and space charge property of MgO/LDPE nanocomposite», *Dielectrics and Electrical Insulation, IEEE Transactions on*, bd. 21, nr. 4, s. 1957–1964, 2014.

[6] T. G. Aakre, T. Ve, og Ø. Hestad, «Conductivity and permittivity of Midel 7131 : effect of temperature, moisture content, hydrostatic pressure and electric field», *IEEE Trns. Dielectr. Electr. Insul.*, bd. 23, nr. 5, s. 2957–2964, 2016, doi: http://dx.doi.org10.1109/TDEI.2016.7736858.

[7] F. Mauseth, M. Amundsen, A. Lind, og H. Faremo, «Water tree growth of wet XLPE insulation stressed with DC and high frequency AC», i *2012 Annual Report Conference on Electrical Insulation and Dielectric Phenomena*, okt. 2012, s. 692–695. doi: 10.1109/CEIDP.2012.6378875.

[8] H. H. Saeternes, J. Aakervik, og S. Hvidsten, «Water treeing in XLPE insulation at a combined DC and high frequency AC stress», i *2013 IEEE Electrical Insulation Conference (EIC)*, Ottawa, ON, jun. 2013, s. 494–498. doi: 10.1109/EIC.2013.6554297.

[9] T. W. Giants, «Crystallinity and dielectric properties of PEEK, poly (ether ether ketone)», *IEEE Transactions on Dielectrics and Electrical Insulation*, bd. 1, nr. 6, s. 991–999, 1994.

[10] J. Ho og T. R. Jow, «Effect of crystallinity and morphology on dielectric properties of PEEK at elevated temperature», presentert på 2013 IEEE

International Conference on Solid Dielectrics (ICSD), 2013, s. 385–388.
[11] D. K. Das-Gupta og K. Doughty, «Dielectric and Conduction Processes in Polyetherether Ketone (PEEK)», *Electrical Insulation, IEEE Transactions on*, bd. EI-22, nr. 1, s. 1–7, 1987, doi: 10.1109/TEI.1987.298955.
[12] D. Das-Gupta, K. Doughty, og D. Cooper, «Charge storage and conductivity in poly ether ether ketone (PEEK)», presentert på 1985 5th International Symposium on Electrets (ISE 5), 1985, s. 334–339.
[13] J. Crank, *The mathematics of diffusion*. Oxford: Clarendon Press, 1975.
[14] C.-H. Shen og G. S. Springer, «Moisture absorption and desorption of composite materials», *Journal of Composite Materials*, bd. 10, nr. 1, s. 2–20, 1976.
[15] C. E. Rogers, «Permeation of gases and vapours in polymers», i *Polymer permeability*, Springer, 1985, s. 11–73.
[16] L. A. Dissado og J. C. Fothergill, *Electrical degradation and breakdown in polymers*, 1. utg. London: Peter Peregrinus Ltd., 1992.
[17] E. J. Kim og Y. Ohki, «Ionic behavior of dc conduction in polyetheretherketone», *IEEE Trns. Dielectr. Electr. Insul.*, bd. 2, nr. 1, s. 74–83, 1995.
[18] Y. Sekii og T. Maeno, «Generation and Dissipation of Negative Heterocharges in XLPE and EPR», *Dielectrics and Electrical Insulation, IEEE Transactions on*, bd. 16, nr. 3, s. 668–675, 2009, doi: 10.1109/tdei.2009.5128504.
[19] A. Campus, P. Carstensen, A. A. Farkas, og M. Meunier, «Chemical defects and electron trapping relevant to cable dielectrics», i *2002 Annual Report Conference on Electrical Insulation and Dielectric Phenomena*, 2002, s. 155–158.
[20] M. Unge, C. Tornkvist, og T. Christen, «Space charges and deep traps in polyethylene—Ab initio simulations of chemical impurities and defects», presentert på Solid Dielectrics (ICSD), 2013 IEEE International Conference on, 2013, s. 935–939.
[21] G. Teyssedre og C. Laurent, «Charge transport modeling in insulating polymers: from molecular to macroscopic scale», *Dielectrics and Electrical Insulation, IEEE Transactions on*, bd. 12, nr. 5, s. 857–875, 2005, doi: 10.1109/tdei.2005.1522182.
[22] A. K. Jonscher, *Dielectric response in solids*. London: Chelsea Dielectrics Press Ltd., 1983.
[23] B. V. Hamon, «An approximate method for deducing dielectric loss factor from direct-current measurements», *Proceedings of the IEE-Part IV: Institution Monographs*, bd. 99, nr. 3, s. 151–155, 1952.
[24] R. L. Blaine, «Thermal Applications Note», *TN048 Polymer Heats of Fusion, TA Instruments, New Castle, DE*, 2002.
[25] E. Ildstad, «Water migration and water treeing in cross-linked polyethylene cables», The Norwegian Institute of Technology (NTH), Trondheim, 1982.
[26] M. A. Grayson og C. J. Wolf, «The solubility and diffusion of water in poly (aryl-ether-ether-ketone)(PEEK)», *Journal of Polymer Science Part B: Polymer Physics*, bd. 25, nr. 1, s. 31–41, 1987.
[27] S. Hvidsten og F. Sætre, «Dielectric response of sPP and XLPE insulations at high temperatures and electric fields», presentert på 2011 Annual Report Conference on Electrical Insulation and Dielectric Phenomena, 2011, s. 695–698.

Torbjørn Andersen Ve was born in Bergen, Norway in 1983. He received the M.Sc. degree in physics in 2008 from the Norwegian University of Science and Technology (NTNU) in Trondheim, and a Ph.D. in electric power engineering in 2021, also from NTNU. He started at SINTEF Energy Research in 2008 and is currently employed there as a research scientist, working with topics such as charge accumulation and transport in solid insulation materials, liquid and gas absorption in polymer materials, and electrical ageing phenomena in polymer insulation.

Øystein L. Hestad was born in Mo i Rana, Norway in 1978. He received the M.Sc. degree in physics in 2003 and the Ph.D. degree in chemistry in 2010, both at the Norwegian university of science and technology (NTNU) in Trondheim. Since 2003 he has worked at SINTEF Energy Research in Trondheim. His research interests include prebreakdown and breakdown phenomena in liquid and solid insulating materials.

Sverre Hvidsten received the M.Sc. in 1992 at the Norwegian Institute of Technology (NTH) in Trondheim. During 1993–1994 he was a researcher at EFI in Norway. In 1999 he gained the Ph.D. in electrical engineering at the Norwegian University of Science and Technology, NTNU in Trondheim. He then joined SINTEF Energy Research, where he currently works as a Senior Researcher. He also participates in CIGRE work.

Author Accepted Manuscript version of the paper by Torbjørn Andersen Ve, Øystein Hestad and Sverre Hvidsten
in IEEE Transactions on Dielectrics and Electrical Insulation, 30 (2024) 501-508, http://dx.doi.org/10.1109/TDEI.2023.3243878